

---

# Compressive Sensing and Reconstruction's Algorithm on Radar MIMO

Randrianandrasana Marie Emile<sup>1, \*</sup>, Randriamitantsoa Paul Auguste<sup>2</sup>

<sup>1</sup>Department of Telecommunication, Antsirabe Vankinankaratra High Education Institute, University of Antananarivo, Antananarivo, Madagascar

<sup>2</sup>Department of Telecommunication, High School Polytechnic of Antananarivo, University of Antananarivo, Antananarivo, Madagascar

## Email address:

emile3marie@gmail.com (Randrianandrasana Marie Emile), rpauguste@gmail.com (Randriamitantsoa Paul Auguste)

\*Corresponding author

## To cite this article:

Randrianandrasana Marie Emile, Randriamitantsoa Paul Auguste. Compressive Sensing and Reconstruction's Algorithm on Radar MIMO. *American Journal of Electrical and Computer Engineering*. Vol. 6, No. 2, 2022, pp. 68-80. doi: 10.11648/j.ajece.20220602.13

**Received:** July 5, 2022; **Accepted:** August 10, 2022; **Published:** August 31, 2022

---

**Abstract:** Two advanced technic appears concerning the digital processing: the detection system RADAR and a compression technic named the Compressive Sensing (CS). This modern acquisition technic combined with reconstruction, offers multiple advantages. This research explains a new technic of acquisition with compression: the Analog to Information Converter (AIC). The standard method uses Analog to Digital converters (ADC). This method named AIC can defeat even the Nyquist Shannon criteria, by using advanced transformation. This article shows the application of compressed sensing MIMO RADAR. Based on the propriety of the signal, we study criteria of mathematics' compressibility, to the choice of the methods, the two algorithm of reconstruction that we use named Matching Pursuit (MP) and Orthogonal Matching Pursuit (OMP). So, we could have compressive sensing with Non-Uniform Sampling that we named CS-NUS on this article. Our contribution consists of using detection of the multiple targets combined with the CS. For multiple targets, we use the Principal Component Analysis (PCA) to send the signal and recover it. The Signal to Noise Ratio (SNR) and Compressive Ratio (CR) permit to conclude that Orthogonal Matching Pursuit offers a best performance than Matching Pursuit. The Matching Pursuit algorithm cited previously gives a good time reconstruction processing but not offers a good quality of reconstruction.

**Keywords:** CS, PCA, Radar MIMO, MP, OMP

---

## 1. Introduction

The Nyquist Shannon sampling theorem is a general rule of sampling for the digital signal processing. In this, the small number for the signal processing could be found.

After new discovery about compression and sparse transform like Discrete Cosine Transform (DCT), Discrete Fourier Transform (DFT) and Discrete Wavelet Transform (DWT), the compressive sensing permit to compress and acquire signal simultaneously. These methods could offer low sampling than Nyquist theorem.

## 2. Signal Radar Processing

In classic RADAR processing, the received power, target

distance could be approximated. It is possible to category the radar in two radars's signal pulse type: The modulated pulse (pulse compression) and the constant frequency pulse and.

### 2.1. Estimation of Received Power

The main propose of the RADAR processing is to find the distance between the target and the radar system. In this, the methodology for understanding how working the radar gives a good benefit in this article. [1].

The equation (1) expresses the power of the reception's signal:

$$P_r = \frac{P_t G_t G_r \lambda^2 \sigma}{(4\pi)^3 (R_t)^2 (R_r)^2} \quad (1)$$

With,

$G_t$ : gain's antenna transmission

$G_r$ : gain's antenna reception

$\lambda$ : Wavelength

$P_r$ : Power on the receiver

$P_t$ : Power on the transmitter

$R_t$ : Distance between the transmitter and the radar

$R_r$ : Distance between the receiver and the radar

To find a target, the radar system should consider the surface of reflecting effective and the range of the target. The quantities of these geometrics patters should be study in the system. On MIMO RADAR, the equation (2) expresses the conditions of all quantities:

$$\left(\frac{P_r}{N} \mid \min\right) \leq \frac{\sigma G^2 P_t}{f^2 R_{\max}^4 (T_a + T_r) B} \times \frac{c^2}{(4\pi)^3} \quad (2)$$

With,

$P_t$ : Generator's power W);

$G$ : Gain's antenna;

$f$  (G H z): Frequency;

$\lambda$  (m ): Wavelength;

$R_{\max}$ : Distance on detection maximum's range;

$\sigma$ : Surface Equivalent of Radar SER;

$\frac{P_r}{N}$ : Signal to noise ratio;

$B$  (H z ): Bandwidth's receiver;

$(T_a + T_r)$ : Temperature of noise concerning the receiver's input in Kelvin.

## 2.2. Distance's Target

The signal like short-transmitted radio pulse goes and returns back to the target in the case of a pulse radar. This case permit to compute the distance by using pulse radar with celerity of propagation  $c$ .

As the distance calculated by radar is like a straight-line, the equation (3) expressed this distance between target and antenna.

$$R = \frac{ct}{2} \quad (3)$$

Where:  $i$ : time of propagation until the radar's pulse go back the MIMO radar.

## 2.3. Constant Frequency Pulse

In conventional radars, this method is the most used in the signal radar. The parameter of pulse could be: rectangular shape, frequency, duration. In this, the equation (4) expressed the constant-Frequency pulse radar MIMO.

$$r(t) = u(t)e^{(2\pi f_c t + \phi)} \quad (4)$$

With,  $u(t)$ : the transmitted signal with compressed envelope.

This envelope could be expressed by the equation (5).

$$u(t) = \begin{cases} A & \text{if } 0 \leq t \leq T \\ 0 & \text{others} \end{cases} \quad (5)$$

$f_c$ : carrier frequency's transmission;

$\phi$ : initial phase.

The manner for choosing the angular  $\phi$  has a big reason for well-determine the code. The initial phase is used for the performance of radar system, the countermeasures of warfare's electronic.

## 2.4. Compression's Pulse

The most of signal processing about the target's detection like sonar, seismic, radar and other system uses the compression's pulse. Indeed, about the radar, the PAPR or Peak Average Power Ratio is minimized and SNR (Signal to Noise Ratio) is maximized by this method.

Two modulations methods could be used: frequency and phase modulation.

### 1. Frequency modulation

Linear Frequency Modulation (LFM) is the easiest methods for this. Taking duration of T-pulse and having a range  $\Delta f$ , the signal varies his carrier frequency linearly. On the pulse compression, the main problem is the presence of sidelobe due to the compression which could degrade the radar's resolution. The solution of this problem is the reduction of this sidelobes by using weighting or filtering.

### 2. Phase encoding

The phase encoding uses the same method of the pulse compression [1-3] but duration's pulse T, should be divided into an identical interval's duration T. At the last, A phase value will be associated with each interval.

The equation (6) expressed the complex envelope having the code's phase:

$$r(t) = \frac{1}{\sqrt{T}} \sum_{l=1}^L r_l \text{rect} \left[ \frac{t - (l-1)t_p}{t_p} \right] \quad (6)$$

Where:

$r_l = e^{j\psi_l}$  and the L: the phase system.

$\psi_1, \dots, \psi_L$ : the phase code associated with  $r(t)$ ;  $t_p = T/L$ .

Finding the codes which is represented as the L phases' sequence is more difficult and could be different for each radar system. So, the possible number for generating a phases' sequence having L length will be unlimited.

## 2.5. MIMO Radar Digital Signal Processing Block

The Figure 1 represents the telecommunication chain of Radar MIMO processing.

The multiple receiver antennas permit to capture all signals. The first block consists of filtering processing to separate the needed signal for the MIMO Radar systems.

The second block consists of the radar processing like specific processing techniques, a radar imaging application, target detection and classification [2].

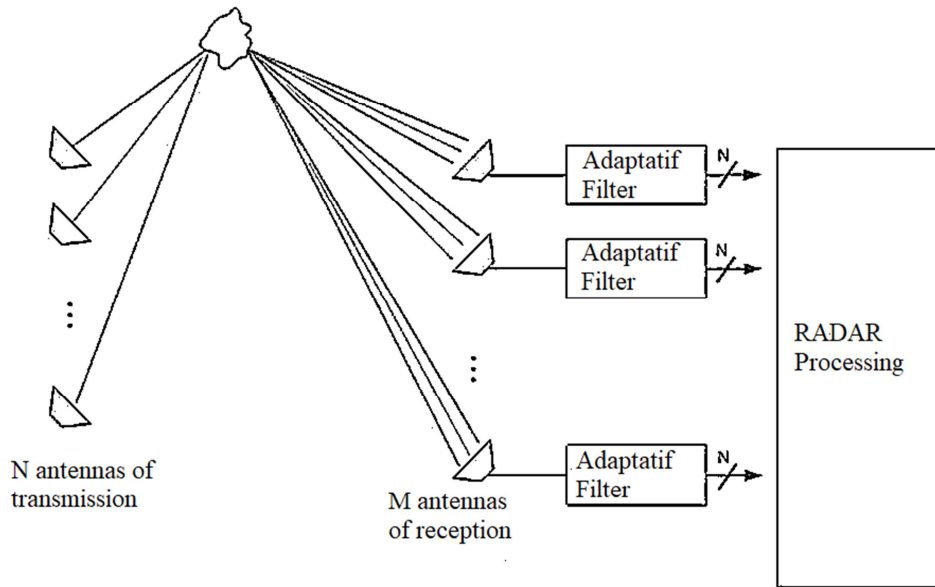


Figure 1. MIMO RADAR processing chain.

2.6. Phased Array Antenna

Many antennas could transmit or/and receive signal of a specific’s direction by controlling the phase of the signal. This technic is named the phased array where the antennas could be placed linearly or planarly.

The best way to represents the space of the antenna is generally a uniform distance. These antennas ’networks could send and receive a signal.

Two antennas could be also used and it’s should be placed in different place allowing the radar to work on bistatic methods. For this case of radar, a small space between the antenna’s arrays permits to have a same SER on each other’s like: In phase-shifted array radars. In this method also, the transmission array permit to sand the same waveform by changing the dephasing offset. [3].

Like mathematics models; let’s study a phased array radar system having  $n_T$  elements ‘transmission and  $n_R$  elements’s reception. The transmitter and receiver are placed linearly uniform and having a space  $d_T$  and  $d_R$  each over.

The equation (7) expressed the received signal.

$$y(t) = \sqrt{\frac{E_T}{n_T}} n_R n_T \gamma' + \eta(t) \tag{7}$$

Were,

$E_T$ : the average total transmitted energy.

$\gamma'$ : the backscatter effect.

$\eta(t)$  is a zero-mean vector of complex.

This parameter could also be expressed like the equation (8) as a random process:

$$\eta(t) = \begin{pmatrix} \eta_1(t) \\ \eta_2(t) \\ \vdots \\ \eta_{n_R}(t) \end{pmatrix} \tag{8}$$

For a suitable filter of the received signal, the signal obtained could be expressed as:

$x(t) = a(\tilde{\theta}) \sqrt{\frac{E_T}{n_T}} x(t)$ , where  $a(\tilde{\theta})$  is the director vector of the transmitter.

In this, the output signal could be sampled at time  $\delta$ .

So, the output becomes:

$$y(t) = \sqrt{\frac{E_T}{n_T}} b^H(\tilde{\theta}') b(\theta') a^H(\theta) a(\tilde{\theta}') \gamma' + \eta(t) \tag{9}$$

Where, the equation (10) expressed  $a(\tilde{\theta}')$  as:

$$a(\tilde{\theta}') = \begin{pmatrix} 1 \\ e^{j2\pi d_T \sin(\tilde{\theta}')} \\ \vdots \\ e^{j2\pi f(n_T-1)d_T \sin(\tilde{\theta}')} \end{pmatrix} \tag{10}$$

And  $b(\theta')$  is:

$$b(\theta') = \begin{pmatrix} 1 \\ e^{-j2\pi d_T \sin(\theta')} \\ \vdots \\ e^{-j2\pi f(n_T-1)d_T \sin(\theta')} \end{pmatrix} \tag{11}$$

The equation (12) expressed the channel matrix of phased array antenna.

$$H = b(\theta') a^H(\theta) \gamma' \tag{12}$$

2.7. Coherent Mimo Radar

The MIMO radar could be also used for a coherent system for transmitting and receiving signals.

The antennas networks array could be co-located and the same or separated network could be used for the transmission and reception function.

The space of each antenna should be study carefully in the case of coherent MIMO radar. The first case is when the space is close enough. All the systems show same characteristic of the target: same SER. Indeed, the Coherent MIMO radar has a big similarity to the phased array radar like on the antenna elements, the deployment pattern. The second case is when the space is large enough, the coherent MIMO radar has a different waveform.

The mathematics model of a coherent MIMO radar system has  $n_T$  transmit elements and  $n_R$  receiving elements.

The equation (13) expressed the received signal by:

$$y(t) = \sqrt{\frac{E_T}{n_T}} H. x(t - \delta) + n(t) \quad (13)$$

With,

$E_T$ : the average total transmitted energy;

$\gamma'$ : the backscatter effect.

$\eta(t)$ : a zero-mean vector of complex random processes.

The received signal has a relation on the input signal to  $x_m(t)$  phased at time instants  $\delta$ .

The equation (14) expressed these matched filters expressed as a vector.

$$\bar{y}(t) = \sqrt{\frac{E_T}{n_T}} \bar{\gamma}' + \bar{\eta}(t) \quad (14)$$

With,

$\bar{y}$ : complex vector having dimensions  $n_T n_R \times 1$ ,

$\bar{\eta}$ : complex noise vector having dimensions  $n_T n_R \times 1$ ,  $\bar{\gamma}'$  expressed by the equation (15) as a complex vector.

$$\bar{\gamma}' = [b^*(\theta') \otimes a^*(\theta')] \quad (15)$$

Where  $\otimes$  denotes the Kronecker product.

In term of distribution, the equation (16) should be verified.

$$b^*(\theta') = \begin{pmatrix} e^{-j2\pi f \delta_{T_1}(\theta')} \\ e^{-j2\pi f \delta_{T_2}(\theta')} \\ \vdots \\ e^{-j2\pi f \delta_{T_{n_T}}(\theta')} \end{pmatrix} \quad (16)$$

$$a^*(\theta') = \begin{pmatrix} e^{-j2\pi f \delta_{T_1}(\theta')} \\ e^{-j2\pi f \delta_{T_2}(\theta')} \\ \vdots \\ e^{-j2\pi f \delta_{T_{n_T}}(\theta')} \end{pmatrix} \quad (17)$$

The equation (18) expressed the channel matrix for the coherent MIMO radar:

$$H = \gamma' b^*(\theta') a^H(\theta) \quad (18)$$

## 2.8. Statistical Mimo Radar

When the space of antennas is really large, each transmitter and receiver pair have a different characteristic of the target indeed about the SER. So, all signals become independents for each pair. The property of this statistical MIMO radar is named angular or spatial diversity. [2, 3].

The model mathematics of statistical MIMO radar system has  $n_T$  transmitters and  $n_R$  receivers.

The equation (19) is expressed the received signal.

$$y(t) = \sqrt{\frac{E_T}{n_T}} H. x(t - \delta) + n(t) \quad (19)$$

With,

$E_T$ : the average total transmitted energy,

$\gamma'$ : the effect backscatter,

$\eta(t)$ : a zero-mean vector of complex random processes.

The received signal has a relation on the input signal to  $x_m(t)$  phased at time instants  $\delta$ .

The equation (20) expressed these matched filters expressed as a vector.

$$\bar{y}(t) = \sqrt{\frac{E_T}{n_T}} \bar{\gamma}' + \bar{\eta}(t) \quad (20)$$

With,

$\bar{y}$ : complex vector having dimensions  $n_T n_R \times 1$ ,

$\bar{\eta}$ : complex noise vector having dimensions  $n_T n_R \times 1$ ,

$\bar{\gamma}'$  expressed by the equation (21) as a complex vector.

$$\begin{pmatrix} Y_{11} \\ Y_{12} \\ \vdots \\ Y_{n_R n_T} \end{pmatrix} = \sqrt{\frac{E_T}{n_T}} \begin{pmatrix} Y_{11} \\ Y_{12} \\ \vdots \\ Y_{n_R n_T} \end{pmatrix} + \begin{pmatrix} \eta_{11} \\ \eta_{12} \\ \vdots \\ \eta_{n_R n_T} \end{pmatrix} \quad (21)$$

The equation (22) expressed the channel matrix for the coherent MIMO radar:

$$H = \text{diag}(b(\theta') \gamma' \text{diag}(a(\theta))) \quad (22)$$

## 3. Materials and Methods

The materials and methods concern indeed about the compressive sensing, the transmission, the reconstruction of signal on reception with CS-NUS.

### 3.1. Compressive Sensing

In the field of digital signal processing (Figure. 2), it is customary to refer to the Nyquist-Shannon theorem to faithfully reconstruct a signal of width spectral and amplitude-limited: This theorem, also known as the sampling theorem, states that the exact reconstruction of a band-limited signal requires that the frequency of sampling is greater than or equal to twice the width of its spectrum (i.e., the difference between the minimum and maximum frequencies it contains) [4].

Except that usually, after this sampling phase, and due to transmission or storage restrictions, a compression step is performed.

One of the most popular compression techniques is sparse decomposition compression: signals can be sparse or compressible in the sense that they have concise representations in bases or well-chosen dictionaries.

Thus, we can cancel a large part of the small coefficients without perceptible loss.

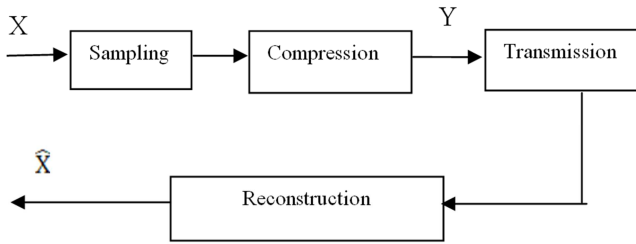


Figure 2. Conventional approach to digital signal processing.

This strategy is adopted by most modern compression standards, especially in the area of image processing, such as JPEG-2000. First a sparse transform is applied to the image, translating the input signal into a vector of coefficients, then this sparse vector is encoded by selecting the most significant coefficients and ignoring the smaller ones. The compressed data Y will then be transmitted and finally reconstructed. This approach works well in many applications.

However, acquiring many samples and then ignoring many of them is extremely expensive. The main idea of compressed sampling is, as its name suggests, to directly capture the data in a compressed form by exploiting the sparse of the signal (Figure 3): instead of generating N samples, the goal is to generating only M measurements ( $M \ll N$ ) such that their acquisition allows efficient reconstruction of the input signal. Thus, compressed acquisition makes it possible to capture a signal at a frequency significantly lower than the Nyquist frequency.

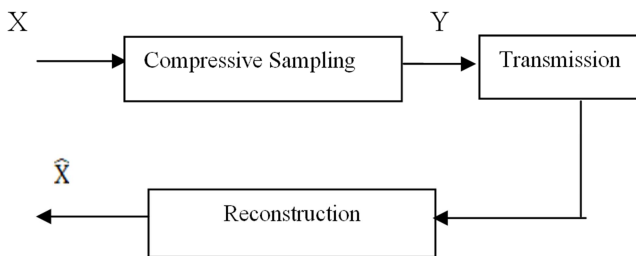


Figure 3. Compressive sensing paradigm.

### 3.2. Signal Acquisition

Mathematically, Compressive Sensing (CS) is defined by [5]:

$$Y = \Phi X + Z \tag{23}$$

Y represents the compressed data that will be digitized by the ADC or Analog digital Converter quantizer, it is formed by M measurements. X is the unknown signal formed by N samples.  $\Phi$  is the matrix of measurement matrix (Gaussian, Bernoulli, Discrete Fourier Transform or DFT etc.) of size  $M \times N$ , with  $N > M$ , modeling a subsampling and Z is an unknown noise term (quantization noise, thermal noise, etc.).

### 3.3. Signal Reconstruction

Reconstruction takes more time and power than acquisition.

For most CS applications, this step is not implemented on the circuit with the step of the acquisition. [6].

According to equation (23), to reconstruct the signal X from the recovered measurements, there are more unknowns than equations ( $N > M$ ). We have in the case of an under-determined system. Mathematically, this system has an infinity of solutions. In order to solve this problem, the CS is essentially based on two notions: the sparse (or the compressibility) of the signal, and the verification of the restricted isometric propriety (RIP) by the measurement matrix (or the inconsistency between the measurement matrix and the basis of sparse).

### 3.4. Sparse and Compressibility

All intelligence resides in a priori knowledge of the signal. In the case of CS, we are interested in sparse or compressible signals. The sparse expresses the idea that the information rate of the signal is smaller than that suggested by its bandwidth.

In CS, the more signal sparse, the lower the number of samples required for its reconstruction. [4, 7].

A signal is K parsimonious in a database or dictionary if it can be described by a small number K of non-zero coefficients in this base / dictionary ( $K \ll M < N$ ). It is expressed by:

$$X = \psi S \tag{24}$$

With S the sparse representation of X such that  $\|S\|_0 \leq K$  and  $\Psi$  is the basis of parsimony of dimension  $N \times N$ .

Equation (25) becomes:

$$Y = \Phi \psi S + Z \tag{25}$$

Few natural signals are sparse: when we talk about sparse in CS, we are actually talking about compressibility. Intuitively, this means that the signals can be represented by a few significant coefficients while the others are close to zero. Figure 4 illustrates the difference between these two concepts.

Mathematically, a signal is compressible if the module of its coefficients sorted in  $\Psi$  follow a decrease in power law:

$$|S_i| \leq C i^{-q}; i = 1, 2, \dots, N \tag{26}$$

Where C is a constant. The larger q is the degradation of the signal and the more compressible the signal will be.

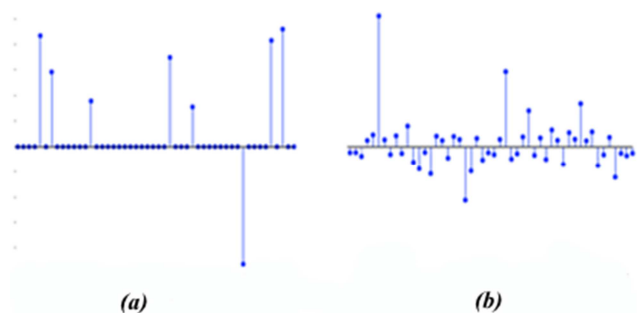


Figure 4. Sparse signal (a) and compressible signal (b).

### 3.5. Restricted Isometry Property (RIP) and Inconsistency

The CS chooses a  $K$ -sparse solution among the possible solutions of the equation (23). The existence of the solution is trivial. On the other hand, its uniqueness and its stability are not guarantees. One of the major contributions of the first work on CS is the definition of the mathematical framework to satisfy the uniqueness and the stability of the  $K$ -sparse solution. For this, other conditions must be considered on the acquisition method.

In particular a condition which ensures a good reconstruction of the data, is to check that the matrix:  $A = \Phi\Psi$  satisfies the restricted isometric property (RIP). [8].

Matrix  $A$  satisfies the RIP of order  $K$  if there is an isometric constant  $\delta_K \in ]0,1[$  such that for any  $K$ -sparse vector, we have the following frame:

$$(1 - \delta_K) \leq \frac{\|AS\|_2^2}{\|S\|_2^2} \leq (1 + \delta_K) \quad (27)$$

$\delta_K$  is the smallest number which ensures this framing for any  $K$ -sparse vector.

Intuitively, the order RIP  $k$  means that the measurement matrix approximately preserves the norm of any  $K$ -sparse vector. The random matrices satisfy the RIP with a very high probability with certain conditions on the number of measurements. For example, it was demonstrated that random matrices with Gaussian or sub-Gaussian inputs satisfy the RIP with a high probability provided that  $M = O(K \log N)$ .

The RIP condition is a sufficient condition to allow the resolution of the equation of CS. It ensures the uniqueness of the solution and its stability for  $\delta_K < \sqrt{2} - 1$ . Unfortunately, RIP is a difficult NP problem. It is difficult to construct matrices satisfying this property with certainty and to verify it. There is another theoretical approach to compressed acquisition based on the notion of the inconsistency between the measurement matrix and the sparse basis.

Consistency between  $\Phi$  and  $\Psi$  is expressed by:

$$\mu(\Phi, \Psi) = \sqrt{(N)} \max_{1 \leq u, j \leq N} |\langle \Phi_u, \Psi_j \rangle| \quad (28)$$

With  $1 < \mu(\Phi, \Psi) < \sqrt{(N)}$  is the set of consistency values between a line of  $\Phi$  and a column of  $\Psi$ . The lower the consistency, the lower the number of measurements required for reconstruction and the greater the compression factor. [9].

Intuitively, low coherence means that the signal which is sparse in  $\Psi$  has a dense representation in  $\Phi$ . An example of two inconsistent bases is the time frequency duality: a Dirac or a peak in the time domain is spread out in the frequency domain. Conversely, a frequency is spread into a pure sine wave in the time domain.

Compressed sampling theory based on this approach states that if we perform  $M$  measurements using linear random projections, i.e., by taking the product of the input signal with a random measurement matrix, then the number of measurements needed to recover  $X$  with a high

probability is:

$$M \geq Cu^2(\Phi, \Psi) K \log(N) \quad (29)$$

In the case where the measurement matrix is completely inconsistent with the sparse basis, the minimum number of random measurements to have a high probability, a good reconstruction is:

$$M \geq \log(N) \quad (30)$$

Note that some random matrices are largely inconsistent with any fixed bases. Indeed, if we choose an orthonormal measurement matrix whose columns are taken in a uniformly random manner then, with a very high probability, the consistency between the measurement matrix and the parsimony basis is of the order of:

$$\sqrt{2 \log N} \quad (31)$$

This is why a Bernoulli matrix, composed of random  $\pm 1$  binary inputs, or a Gaussian matrix are highly inconsistent with any basis of sparse.

### 3.6. Greedy Reconstruction Algorithms

Several reconstruction techniques have been explored to recover the sparse solution from a reduced number of measurements. Greedy algorithms are signal processing techniques, called sparse decomposition techniques. The idea is to iteratively construct a sparse approximation of the signal. [10].

Greedy algorithms build from an initial value  $X_0 = 0$ , at each iteration, an approximation  $X_k$  signal and evaluates a residual error. The operation is repeated until a stop criterion set by the user.

#### 1. Matching Pursuit (MP)

We have a measurement vector  $Y$  and a matrix  $A = \Phi\Psi$  and we want to write  $Y$  as a linear combination of elements  $a_i$  of  $A$  or at least approach  $Y$  by such a linear combination, in other words reconstruct the signal  $X$ . The MP proposes a simple approach: At the start, the residue  $r$  is initialized with the measurement vector  $Y$  and the approximation of the signal  $\hat{X}$  by a zero vector such that  $r_0 \leftarrow Y$  and  $\hat{X} \leftarrow 0$ .

At each iteration  $k$ , the algorithm will have to choose the column  $a_i$  of the matrix  $A$  most correlated to the measurement vector  $Y$ . The standard MP algorithm uses the dot product as the correlation function.

$$\lambda_k = \operatorname{argmax} |\langle r_{k-1}, a_i \rangle| \quad (32)$$

Where,

$\lambda_k$  is the index of the selected column;

$r_{k-1}$  is the residual of the previous iteration;

$a_i$  represents the column of matrix  $A$  with  $1 \leq i \leq N$ , they are also called atoms.

Then, the MP constructs a new approximation of the signal by adding to  $\hat{X}_k$  the projection of the residue on  $a_{\lambda_k}$ , then it updates the residual signal (this is called the residue)  $r_k = Y - Y_k$ .

$$\widehat{X}_k = \widehat{X}_{k-1} + \langle r_{k-1}, a_k \rangle \cdot a_k \quad (33)$$

Where,

$\widehat{X}_{k-1}$  represents the approximation of the signal obtained during the previous iteration;

$r_k$  is the column of the selected matrix A.

The process is repeated until the signal is broken down satisfactorily, that is, until the stop condition is met. The criterion for stopping this algorithm may be:

- a) A residual error below a given threshold
- b) A maximum number of iterations;
- c) A criterion of calculation time, memory, etc.

The description of the MP algorithm is as follows:

*Algorithm 1.*  $x = MP(y, \phi)$ :

```

k = 1, // initialization
ε0 = y, dictionary D0 = ∅
k = 0
repeat
for m ← 1, M do
Cmk ← ⟨ek-1, φm⟩ // Scalar products
end for
mk ← arg maxm |Cmk| // Selection
Dk ← [Dk-1, φmk] // Actif dictionary
xk ← [xk-1; Cmkk] // Actif coefficient
ek ← ek-1 - Cmkk φmk // Residue
k ← k + 1
until (residual error < threshold or k >
max_iteration or memory > max_memory )
    
```

## 2. Orthogonal Matching Pursuit (OMP)

In the OMP we also select the atoms  $a_i$  one by one but with each new atom selection, we choose as a new approximation the orthogonal projection of the starting signal Y on the subspace generated by all of these atoms ( $a_j$  for  $j = 1 \dots k$ ). This update rule makes that after k iterations,  $\forall i = 1 \dots k, \langle a_i, r_k \rangle \geq 0$ ,

So, with each iteration a new atom will be selected. Thus, the OMP performs a maximum of M iterations for a measurement vector Y having M elements.

The description of the OMP algorithm is as follows:

*Algorithm 2.*  $x = OMP(y, \phi)$ :

```

k = 1, // initialization
ε0 = y
D0 = ∅ // dictionary
k = 0
Repeat
for m ← 1, M faire
Cmk ← ⟨ek-1, φm⟩ // Scalar products
end for
mk ← arg maxm |Cmk| // Selection
Dk ← [Dk-1, φmk] // Actif dictionary
xk ← arg minx ||y - Dkx||2 // Actif coefficient:
ek ← y - Dkxk
k ← k + 1
until (residual error < threshold or k >
max_iteration or memory > max_memory )
    
```

## 3.7. Compressive Sensing with Non-uniform Sampling Architecture (CS-NUS)

It is an architecture suitable for sparse signals in the frequency domain ( $\psi = DFT^{-1}$ ).

It is based on the principle of time-frequency duality: Indeed, the time and frequency domains are inconsistent with each other. So, for a sparse signal in the frequency domain and applying the probabilistic approach of compressed acquisition, it suffices to acquire samples in the time domain in a non-uniform and arbitrarily spaced way. [11-13].

The idea behind the NUS is schematized in Figure 5. For the sake of didacticism, suppose that there is an ADC which samples the input signal at the Nyquist frequency. A Pseudo-Random Bit Sequence (PRBS) controls which of these samples are collected and which are ignored. Of all the N samples at the Nyquist frequency, only  $M \ll N$  are collected.

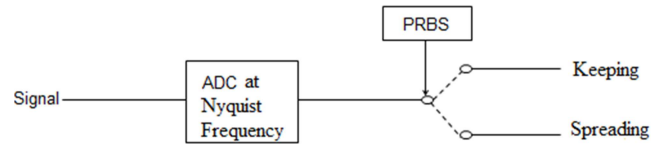


Figure 5. Conceptual diagram of the NUS architecture.

The aim of the CS is to obtain an average sampling frequency lower than the Nyquist frequency. Also, in practice, non-uniform sampling based on the principle of compressed sampling (CS-NUS) chooses samples arbitrarily spaced by an integer number of clock periods at the Nyquist frequency.

The measurement matrix corresponding to this architecture is a rectangular matrix of  $M \times N$  presented by  $\Phi_{NUS}$ : in each row of the measurement matrix, there is only one coefficient not zero and equal to 1. The location of this coefficient in the line is random, this allows to define a sample among N which will be taken in a random way. An example of measurement matrix  $\phi_{NUS}$  is illustrated by:

$$\phi_{NUS} = \begin{pmatrix} 1 & 0 & 0 & 0 & 0 & \dots & 0 \\ 0 & 0 & 1 & 0 & 0 & \dots & 0 \\ 0 & 0 & 0 & \ddots & 0 & \dots & 0 \\ 0 & 0 & 0 & 0 & \dots & 1 & 0 \end{pmatrix}_{M \times N} \quad (34)$$

## 4. Results and Discussion

### 4.1. Analysis of Coherence and Measurement Matrices

After simulation the consistency between the matrix  $\Psi_{DFT^{-1}}$  and the measurement matrices could be represented on the figure 6.

The Figure shows multiple parameters like:

1. The matrix  $\phi_G$  having components giving from a random process like Gaussian with zero mean and  $1/M$  variance.
2. The matrix  $\phi_{B[0,1]}$  having components giving from random process like Bernoulli and which could have values between  $\{0, 1\}$ .
3. The measurement's random demodulator named by  $\phi_{RD}$ .

4. The measurement's matrix Non-Uniform Sampler  $\phi_{NUS}$ .

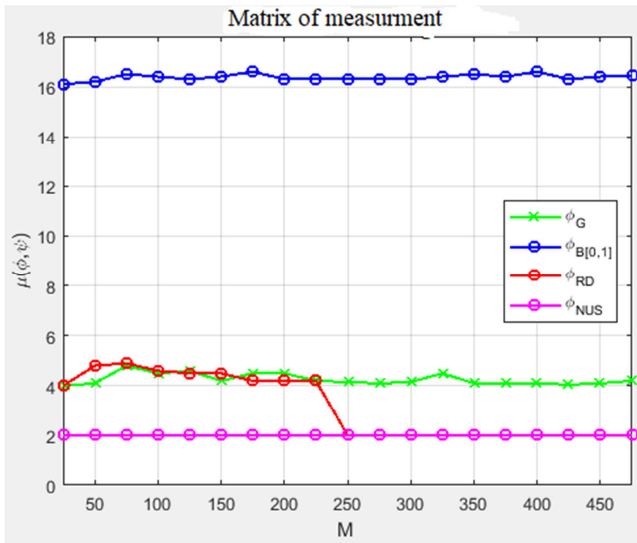


Figure 6. Measurement's matrix  $\phi$  and coherence  $\mu$  between  $\psi_{DFT^{-1}}$ .

On the MATLAB simulation, the parameters values taken for having these results are  $N = 500$  and  $M$  between 25 to 475. The two coherences: at the first between the Gaussian the matrix and the matrix  $\psi_{DFT^{-1}}$ ; at the second between Bernoulli random matrices and the matrix  $\psi_{DFT^{-1}}$  looks like a curve similarly constant and which is independent of the  $M$ 's value. This constant is around 4.5. When  $M$ 's values are high, the consistency between the matrix  $\phi_{RD}$  and the matrix's base sparse  $\psi_{DFT^{-1}}$  take value nearby 2. Noticed that the value 1 is the of consistency's lower bound. The three curves converge from  $M = 100$ .

Even without random columns' permutation and random generation values of blocks which forming the diagonal doesn't change the consistency between  $\psi_{DFT^{-1}}$  and the matrix's measurement.

The consistency for the  $\phi_{NUS}$ , is near the constant with value 2.

In Non-uniform sampling, having signal lower is due to the inconsistency between time and frequency.

The matrix's measurement modeling the under-sampling looks like the canonical matrix. The inconsistent exist between the  $DFT^{-1}$  and this matrix. [14, 15].

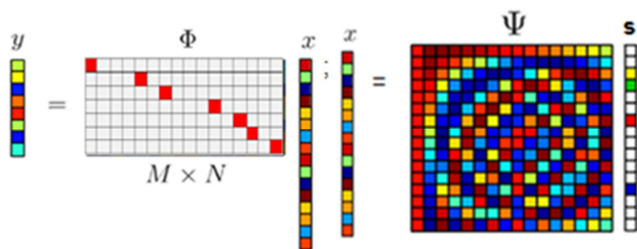


Figure 7. Architecture with NUS measurement's matrix  $\phi$ .

The architecture has a random row coefficient location which gives the property with sampling among  $N$  by using a random process. In this article, we use this method for generating the measurement matrix like on the Figure 7. [15].

4.2. Reconstruction Algorithm with Quality Evaluation and Metrics

It's possible to measure the distortion between the origin signal  $x$  and the reconstructed signal  $\check{x}$  for evaluation the quality of the reconstruction. The equation (35) and (36) expresses the evaluation's criteria named respectively: "Percentage Root-mean-square Deviation (PRD)" and the "Signal to Noise Ratio (SNR)" [15]:

$$PRD[\%] = \frac{\|x - \check{x}\|_2}{\|x\|_2} \times 100 \quad (35)$$

$$SNR[\text{dB}] = 20 \log_{10} \frac{\|x - \check{x}\|_2}{\|x\|_2} \quad (36)$$

With,  $x$ : the original  
 $\check{x}$ : the reconstructed signal.

The quality of reconstructed signal will be evaluated by the PRD value, the Compression Ratio (CR) and the Compression Factor (CF) expressed respectively by the equation (37) and (38).

$$CR[\%] = \frac{N-M}{N} \times 100 \quad (37)$$

$$CF = \frac{N}{M} \quad (38)$$

With,  $M$ : the rows' numbers of the measurement matrix  $\phi$   
 $N$ : the columns 'numbers of the measurement matrix  $\phi$ .

For the simulation, sinusoidal signals is taken from the MATLAB database The signals will be divided into blocks of consecutive samples named by  $N$ . On the radar emitter, The NUS measurement matrix permits to the signal to be compressed. Then, on the radar receiver, the block of reconstruction is a processing bloc permits to have a signal similar of the signal sent. In this, two algorithms of reconstruction are proposed. After the full signal reconstruction, the criteria defined previously are valuated like: PRD and SNR.

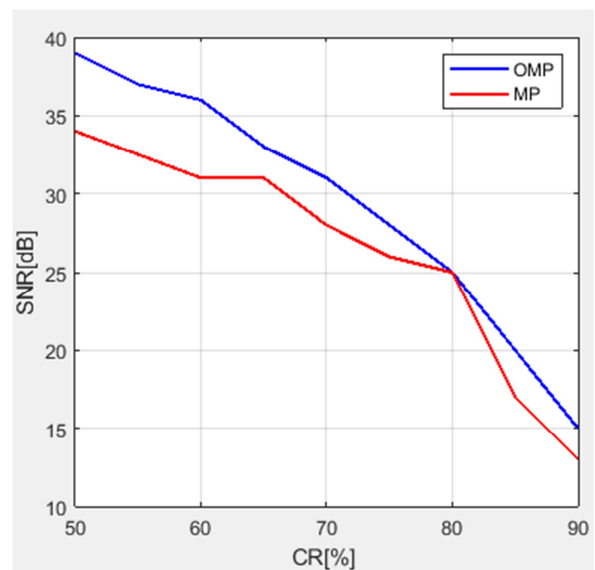


Figure 8. SNR and CR using sinusoidal signals.

The Figure 8 explains that's with it is possible to modify the SNR for each transmission. If we fixed the SNR, for example 30dB, the OMP offers a good compressive ratio than MP. In the same condition ratio of transmission, it's possible to have a big compression ratio using OMP than MP.

For any constant compressive ratio, for example 70%, the SNR of MP is not good than OMP. So, with a fixed Compressive ratio, the OMP could support more bad condition ratio than MP.

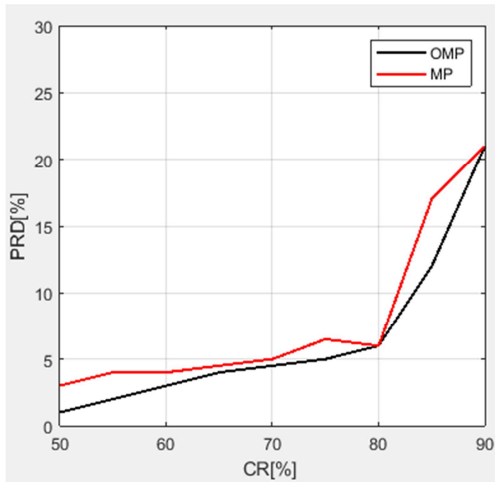


Figure 9. PRD as a function of compression ratio for sinusoidal signals.

The Figure 9 shows the similarity of the reconstructed signal and signal sent comparing to the compression ratio. If the PRD is near zero, the two signals are quasi-identical. So, the OMP offers a good quality of reconstruction than MP for each compression ratio.

Figure 8 and Figure 9 show the curve of SNR and PRD expressed by the compression ratio. Using high compression rate permits the degradation of the reconstructed signal. We got a higher SNR and a lower PRD. Due to the parsimony of sinusoidal, the performance could be a bit best than classic signal.

### 4.3. Norm $L_p$

Let's define a discrete signal with finite length modeling as vectors in a dimension N of Euclidean space represented by:  $(\mathbb{R}^N: X = X_1, X_2, \dots, X_N)$ . It's possible to express the norm of  $L_p$  like the equation (39) [16]:

$$\|X\|_p = (\sum_{i=1}^N |X_i|^p)^{1/p} \in [1, \infty[ \quad (39)$$

For measuring the signal's strength or an approximation's margin error, standards could be used primarily. It's very important to choose this standard  $L_p$  because its influences the characteristic of the resulting approximation error. A high values of "p" conducts to the distribution of the error more evenly among the signal coefficients. A low value conducts to an error which is more unevenly distributed. So, it's will tend to have a good sparsity.

So, the most general evident is to use the norm  $L_1$  to reconstruct signals 'parsimonious'.

### 4.4. Radar Signal and His Compressibility

For the compressibility of the signal, a transform should be used for having parsimony. It could be divided in two categories:

1. The bases / dictionaries which need to study the signal for long training examples.
2. The usual frequency and wavelet transform (Fourier, identity, wavelet, etc.).

Multiple domains like signal's compressibility in the time domain ( $\psi = \text{Identity}$ ), in the frequency domain ( $\psi = \text{DFT}^{-1}$ ) and in the time-frequency domain (wavelet domain which has a waveform close to the signal waveform) permits to study the compressibility [15].

Note that, the condition for having a compressible signal in a specific domain consists for decreasing rapidly the coefficients' moduli ( $|S_i|$ ) which is sorted in  $\psi$ . Then the signal is more compressible when the decay is faster.

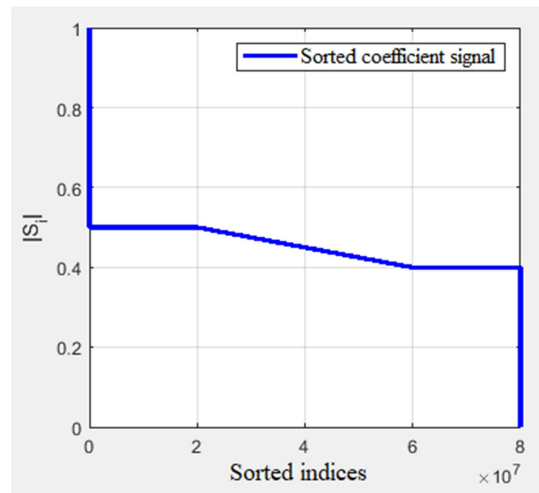


Figure 10. Compressibility of signal radar on time domain.

In all specifics (time, time-frequency using Daubechies10 wavelet, frequency) domains, the radar signal compressibility will be represented on the Figures 10, 11, 12 and 13.

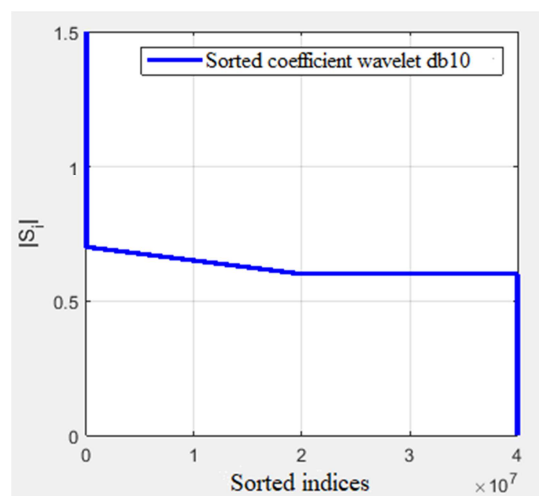


Figure 11. Radar signal compressibility on frequency time having a dB10 wavelet.

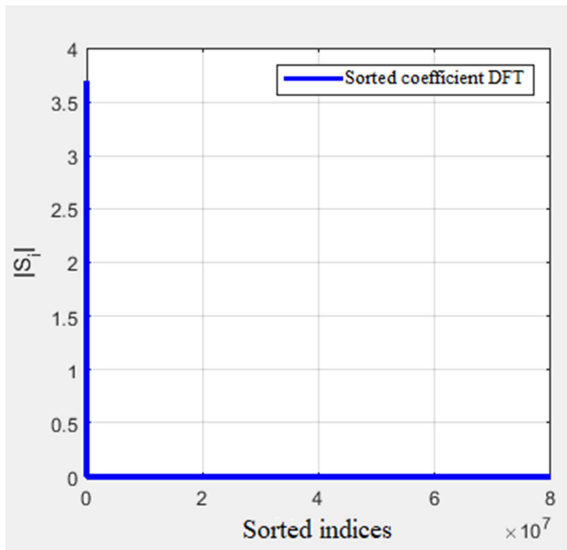


Figure 12. Radar signal compressibility on the frequency domain.

Our simulation is tested at 1 second of data having 80 million of sampling.

All Figure show that when the ( $|S_i|$ ) decrease near zero in all specific domain (the time domain; the time domain and frequency), it will be slow and small than the decay in the frequency domain. Then, in the frequency domain, the Radar signal is more compressible.

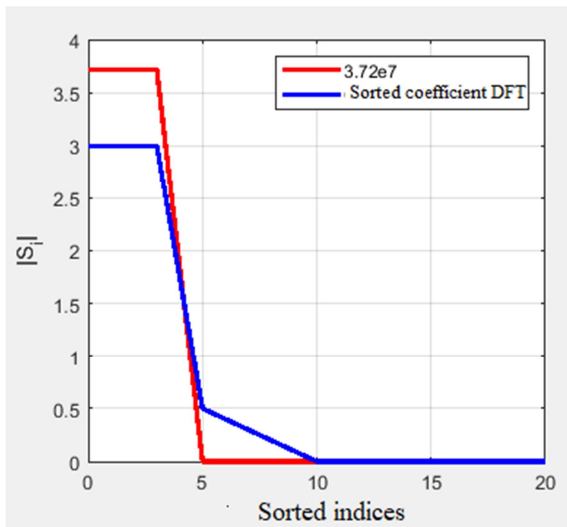


Figure 13. Radar signal Compressibility in the frequency domain and  $|S_i|$ .

The Figure 13 shows the relation between the Fourier's module and the coefficients sorted by a decrease power law: When  $|S_i| = 3.72i^{-5}$  like on the same figure; with  $i$  is the coefficient's index sorted in the  $DFT^{-1}$  transform; the curve decreases also.

#### 4.5. Compressive Sensing Radar and Multi-Targets

##### 1. Schematic illustration with two targets radar

The radar MIMO system has a source  $S$  which emits a propagation wave having frequency  $f$ , and propagates in space for reflecting partially on the targets  $C_1$  and  $C_2$  at a distance  $R_1$  and  $R_2$ . In this, the Figure 14 represents the

equivalent radar surface  $SER_1$  and  $SER_2$  of the two targets.

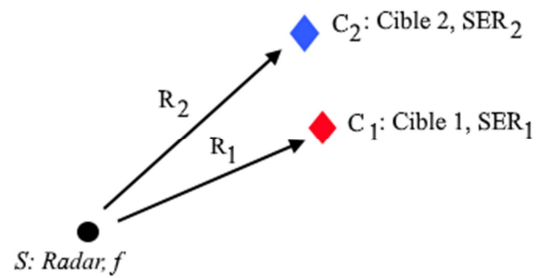


Figure 14. Schematic of the study in general.

The results depend on the nature of frequency which could be separatee in two cases: Very High Frequency (VHF) and High Frequency (HF).

##### 2. Very High Frequency (VHF)

The parameters the VHF case could be shown in the Table 1.

Table 1. VHF's parameter.

Number of target $n$	2
PRI's value	100 $\mu$ s
Frequency $f$	50Mhz
Position relative $R$	50 m
Target position 1 $R_1$	25 m
$SER_1$	1 $m^2$
Target position 2 $R_2$	35 m
$SER_2$	2 $m^2$
Windowing	Hamming

One of the parameters is the Period Repetition of Impulsion (PRI).

In signal MIMO radar processing, for the interest of the limited length, windowing is used.: indeed, about the limited duration of the real signal. Then, a finite number of points is done on computation processes. To show a signal in a time 's finite period, it should be multiplied by function named by an observation window.

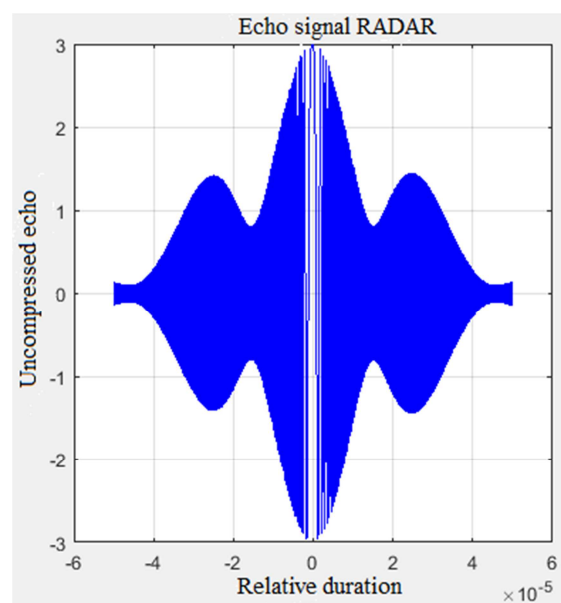


Figure 15. Signal's VHF echo.

By using the parameter 1; the result on Figure 16 and Figure 17. Firstly, the Figure could be interpreted by separating it in two curves: on the left of zero value for illustrating the radar signal's VHF sent and on the right of zero value for showing the radar signal's VHF echo without compression. Secondly, Figure 17 represents the same curve but using a simple compression.

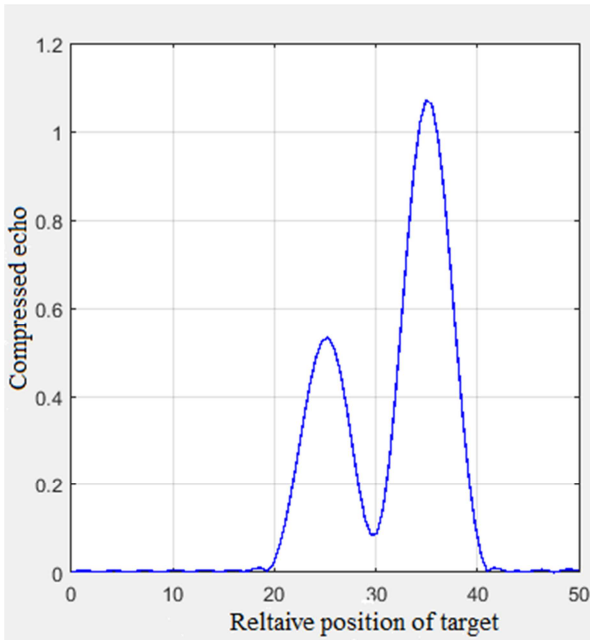


Figure 16. Signal's VHF echo after compression.

The two pics on the figure represents the presence of two targets that we named  $C_1$  and  $C_2$ .

3. High Frequency (HF)

Like on VHF, the HF's parameters parts could be found in the Table 2.

Table 2. HF's parameters.

<b>Number of target <math>n</math></b>	<b>2</b>
PRI's value	100 $\mu$ s
Frequency $f$	6Mhz
Position relative $R$	50 m
Target position 1 $R_1$	25 m
$SER_1$	1 $m^2$
Target position 2 $R_2$	35 m
$SER_2$	2 $m^2$
Windowing	Hamming

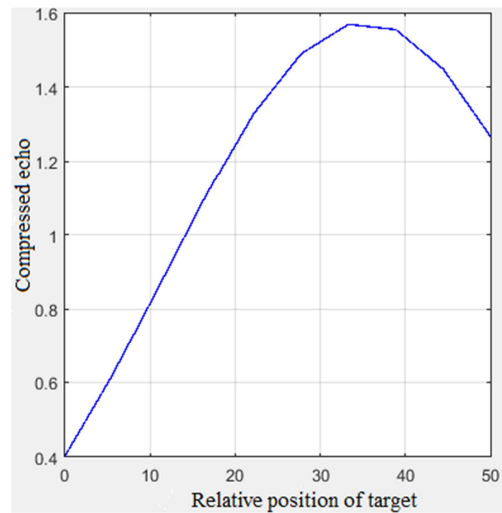


Figure 18. Signal's echo HF after compression.

By using the parameters 2, two results appear after simulation like on Figure 17 and Figure 18. The first figure represents the radar signal's echo HF and the second represents the result of the radar echo HF after simple compression. The methods in this article concern a sampling based on condition's Nyquist-Shanon and pulse compression.

Instead of Figure 16, the two targets  $C_1$  and  $C_2$  doesn't appear on the curve due to low frequency. In the two Figures 17 and 18, Hamming windowing permit to have an observation of window function.

4. Proposed solution and numerical simulation

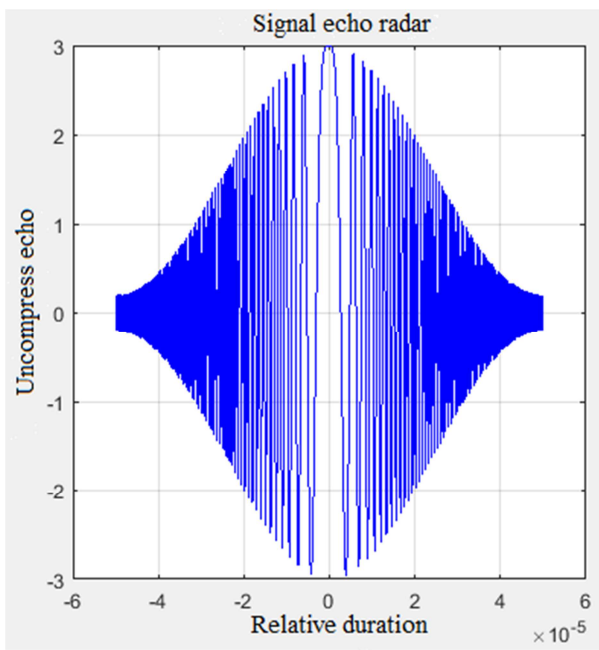


Figure 17. Signal's echo HF in low frequency.

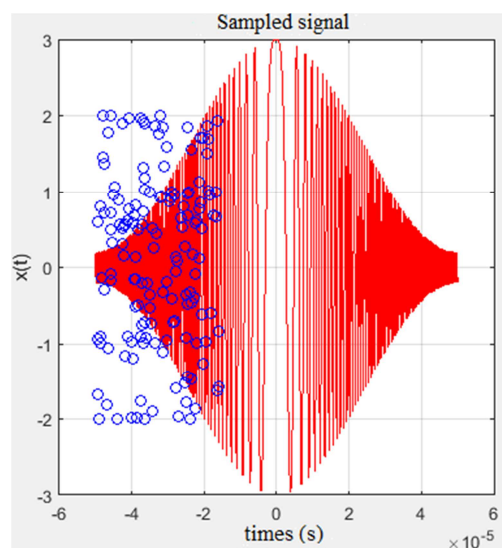


Figure 19. Echo signal sampling.

Like proposed solution, the CS will be applied for the radar signals and the simulation keeps the same value like in the previous parameter 2 so his frequency should be low. (For  $N = 1028$  and  $M = 171$ ). This sampling method is represented in the Figure 19 and is colored on red. So, the red curve represented the CS-NUS instead of using a classic sampling.

The result in Figure 20 shows that, the Sparse Fourier Transformation (SFT) concerns generally a technique using at NUS methods. It is possible to compute outputs and take the advantage of the low complexity compared with the method which uses Fast Fourier Transformation (FFT). Using SFT, the data streams processing could be 10 to 100 time faster than FFT. So, on FFT; we should process all the sequences and the non-zero values gives desired output.

Indeed, a same area regroups the similarity: at the beginning and the end for representing the low frequency. Without SFT, this sparse representation couldn't be obtained.

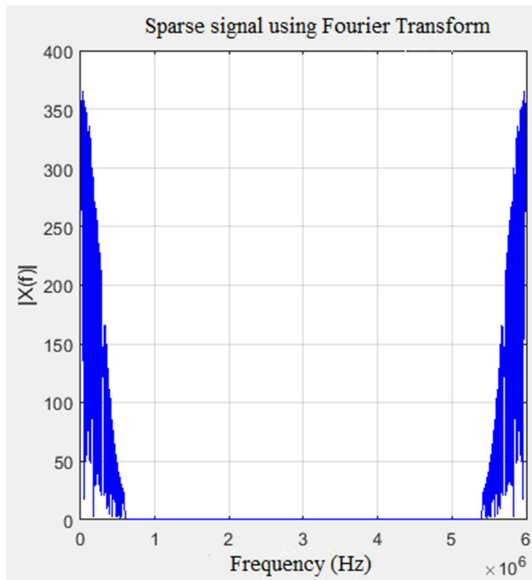


Figure 20. Sparse representation of the Fourier transform.

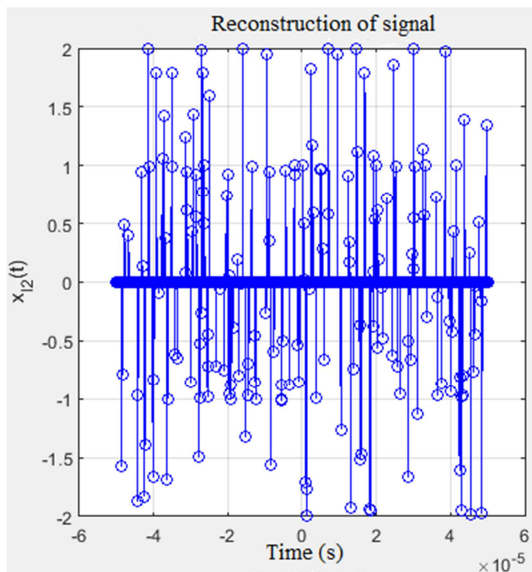


Figure 21. Signal's reconstruction.

The Figure 21 represents the reconstructed signal on the receiver.

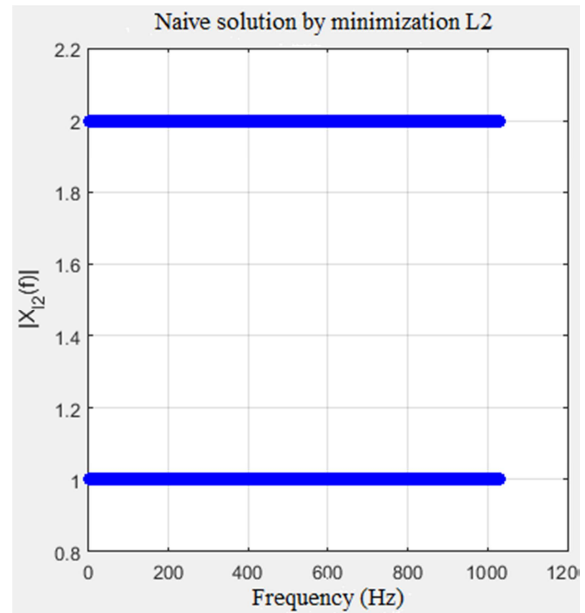


Figure 22. Minimisation  $L_2$  naïve solution.

Different ways could be done for analyzing a data set made up of P signals. Our solution groups all components under a technic named by Component Analysis. Noticed that; in this, components are represented like synonym of atom.

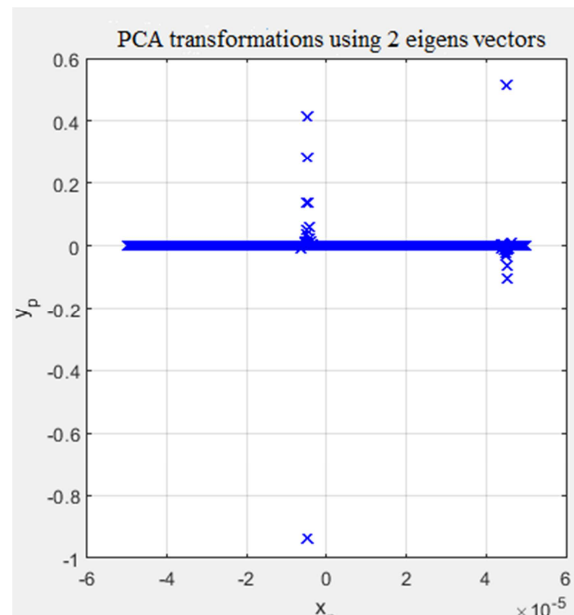


Figure 23. PCA transform with 2 eigenvectors.

Respectively, like summarize, the Figure 19 until 24 shows the echo signal sampled on radar, sparse representation by using Fourier transform, reconstruction's signal, naïve  $L_2$  minimization solution, the transformation using PCA (Principal Component Analysis) with 2 eigenvectors and the OMP reconstruction with approximate solution of  $L_1$ . The NUS's stages architecture are illustrated in these all figures.

Like results shown in Figure 22, proposed solutions with  $L_2$  the minimization have the same as those of the values of  $SER_1$  et  $SER_2$  i.e.  $|X_{L_2}(f)| = \{1,2\}$ . Shown in Figure 24 by using the  $L_1$  approximate solution, this figure represents two sharp pulses for illustrating the numbers of targets named by:  $C_1$  and  $C_2$ . Instead of the simple method represented in Figure 18, it is not possible to distinguish the two targets from these pulses. So, this technique of compressed acquisition named differently by compressive sensing has more advantages indeed about the reconstruction and precision in the sampling domain even the frequency used is low.

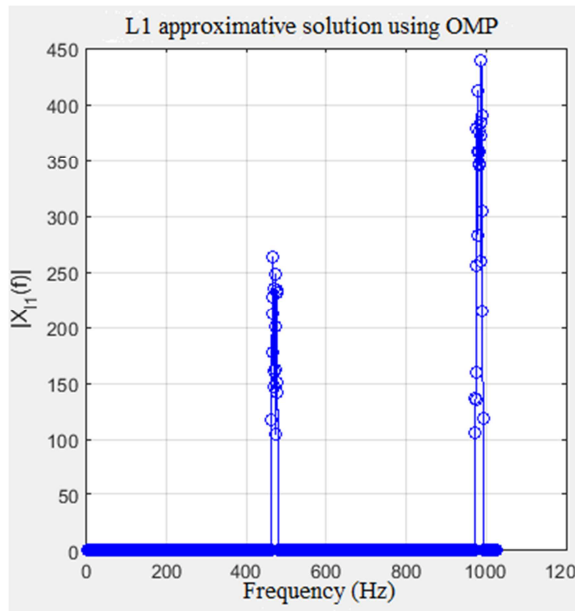


Figure 24. OMP reconstruction with approximate solution of  $L_1$ .

## 5. Conclusion

Our research permit to conclude that using Compressive Sensing doesn't need to invest a lot of resources. Most of transmitted signal are anyway zero. On Radar MIMO, it could reduce power transmission for the multiple targets. This technique needs mathematical condition to be satisfied like: propriety signal, compressibility, matrix measurement. After acquisition, two greedy algorithms MP and OMP are used to reconstruct the signal. The OMP reconstruction is the most robust. It could be used with high CR and good similarity of signal with low PRD. Using CS, the sampling could be lower than Nyquist-Shannon. For multi-targets, the VHF could be reconstructed without new technics. For the HF, PCA could be done for the reconstruction of signal.

## References

- [1] N. Levanon, E. Mozen, RADAR signal, John Wiley and Sons Inc, 2004.
- [2] N. Pandey, Beamforming in MIMO Radar, Department of Electronics and Communication Engineering National Institute of Technology Rourkela 2014.
- [3] Curry, G. R., Radar System Performance Modeling, Artech House, Norwood, 2001.
- [4] M. Lustig, David L Donoho, J. M Santos, John M Pauly, Compressed sensing mri, IEEE Signal Processing Magazine, 2008.
- [5] M. A Davenport, Marco F Duarte, Yonina C Eldar, Gitta Kutyniok, Introduction to compressed sensing, Preprint, 2011.
- [6] E. Candes, J. Romberg, Sparsity and incoherence in compressive sampling, Inverse problems, 2007.
- [7] S. Qaisar, R. Muhammad Bilal, Compressive sensing: From theory to applications, a survey. Journal of Communications and networks, 2013.
- [8] S. G Mallat, Z. Zhang, Matching pursuits with time-frequency dictionaries, IEEE Transactions on signal processing, 1993.
- [9] Y. Chandra Pati, R. Rezaifar, Orthogonal matching pursuit: Recursive function approximation with applications to wavelet decomposition. In Signals, Systems and Computers, IEEE Transactions on signal processing, 1993.
- [10] M. A Lexa, M. E Davies, J. S Thompson, Reconciling compressive sampling systems for spectrally sparse continuous-time signals, IEEE Transactions on Signal Processing, 2012.
- [11] M. Mishali, Yonina C Eldar, From theory to practice: Subnyquist sampling of sparse wideband analog signals; Selected Topics in Signal Processing, IEEE Journal of, 2010.
- [12] E. Candes, Sparse Representations for Radar, URL: <http://www.raeng.org.uk/publications/other/>.
- [13] J. Wang, S. Kwon, P. Li, B. Shim, Recovery of sparse signals via generalized orthogonal matching pursuit, A new analysis. IEEE Transactions on Signal Processing, 2016.
- [14] S. Rapuano, Analog-to-information converters research trends and open problems, In 2016 26th International Conference Radioelektronika, 2016.
- [15] Ankit Kundu, Pradosh K Roy «Sparse signal recovery from nonadaptive linear measurements», 2013.
- [16] SparseLab, URL: <https://sparselab.stanford.edu/>.